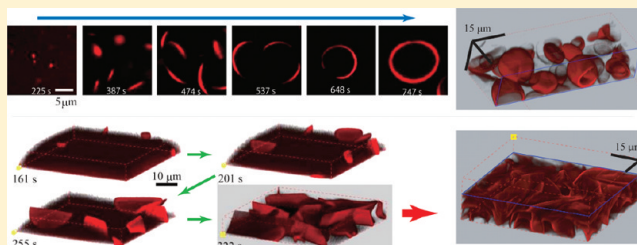


3D Structure of Lamellar Domains in a Surfactant Solution below the Krafft Temperature

Youhei Kawabata,* Hirohito Yashima, and Tadashi Kato

Department of Chemistry, Tokyo Metropolitan University, Hachioji, Tokyo 192-0397, Japan

ABSTRACT: We have studied the 3D structure of lamellar domains in aqueous solutions of nonionic surfactant $C_{16}E_6$ and $C_{16}E_7$ below the Krafft temperature by means of confocal microscopy. A new morphology of lamellar domains has been found in the $C_{16}E_6$ system, which is the network of lamellar domains. In the $C_{16}E_7$ system, we have confirmed that the spherical vesicles have a hollow including excess water. Furthermore, we have investigated the initial formation process of lamellar domains in those two systems. It has been found that initial lamellar domains of both systems are tiny and plate-like and that the domains are gradually curved in the $C_{16}E_7$ system, while in the $C_{16}E_6$ system, they spread to fuse together and form networks.



INTRODUCTION

In aqueous surfactant solutions, amphiphilic molecules self-aggregate to form various kinds of structures, such as micelles, hexagonal, lamellar, and cubic phases. These structures have been investigated from the viewpoint of the self-assembled nanostructure and solubilization for the past several decades, and their structural and physical properties have been gradually clarified. On the basis of the studies, these structures are applied to various kinds of fields, such as pharmacy and material sciences. On the other hand, many unsettled problems still remain, which include nonequilibrium phenomena in the surfactant solutions. One of the matters is the Krafft phenomena, which is the melting of hydrophobic parts of surfactants.^{1,2} The Krafft temperature is one of the important parameters that measure the performance of the surfactants. Generally, in ionic surfactant solutions below the Krafft temperature, hydrated solids of surfactants, the so-called “ α -gels” or coagels, which consist of lamellar crystals, are deposited, and surfactants are much less soluble in water than those above the Krafft temperature. Therefore, most surfactants are usually used above the Krafft temperature in industrial fields. From the viewpoint of fundamental science, it has been reported that the Krafft transition involves some nonequilibrium phenomena.^{3,4} In our previous study,^{5,6} we have investigated the structural phase transition from the micelle to lamellar gel phase (L_g) and the morphologies of lamellar domains by means of optical microscopy and small-angle X-ray scattering (SAXS) in order to clarify the mechanism of the Krafft transition.

We have found new morphologies of the lamellar domains in the hydrated solids below the Krafft temperature in the $C_{16}E_7$ /water and the $C_{16}E_6$ /water systems ($C_{16}E_m$ ($m = 6$ or 7) is the abbreviation of $C_{16}H_{33}(OC_2H_4)_mOH$), as shown in Figure 1. In the $C_{16}E_7$ system, it has been found that multilamellar vesicles with a size of 2–5 μm that have a hollow including excess water

are formed and that the spherical shells consist of 100–150 bilayers. In the $C_{16}E_6$ system, on the other hand, lamellar domains are randomly arranged and form network-like structures. These dramatically different morphologies between the two systems might be due to the feature of bilayers and those stacked lamellar domains. However, the optical microscope images of the $C_{16}E_6$ system suggest string-like lamellar domains, which makes it difficult to imagine how the lamellar domains arrange in three-dimensional space.

In this work, we investigate three-dimensional (3D) structures and formation processes of these lamellar domains, especially in the $C_{16}E_6$ and $C_{16}E_7$ systems, by means of confocal microscopy (CFM), in order to inspect the difference in morphologies between $C_{16}E_6$ and $C_{16}E_7$ systems. Especially for the $C_{16}E_6$ system, we validate the optical microscope images of string-like lamellar domains observed from the optical microscopy experiments in the $C_{16}E_6$ system. Furthermore, we discuss the origin of those morphological differences based on the results of the wide-angle X-ray scattering experiments, which gave us information of the bilayer structures in-plane, and the theory for vesicle formation using the elastic and line tension energies.^{7,8}

EXPERIMENTS

Samples were prepared by mixing $C_{16}E_6$ or $C_{16}E_7$ with D_2O so that the concentration became 10 wt %. The surfactants were purchased from Nikko Chemicals, Inc. in crystalline form and used without further purification. Deuterated water (D_2O of 99.9 atom %D) purchased from Isotec, Inc. was used after bubbling of nitrogen to avoid oxidation of the ethylene oxide

Received: October 29, 2011

Revised: January 9, 2012

Published: January 10, 2012

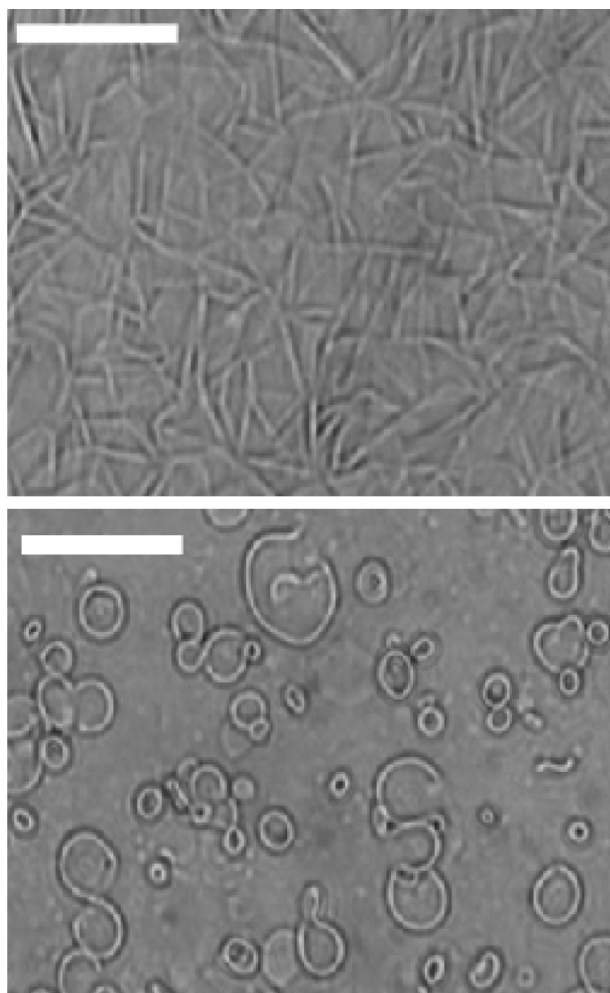


Figure 1. Optical microscope images in phase contrast mode at 60 min after temperature quench in the $C_{16}E_6$ (upper) and $C_{16}E_7$ (lower) systems. The scale bar is 10 μm . In the $C_{16}E_6$ system, lamellar domains are randomly arranged. On the other hand, in the $C_{16}E_7$ system, multilamellar vesicles with a size of 2–5 μm are formed.

group of surfactants.⁹ The reason for using deuterated water is that the phase diagram was made for the $C_{16}E_7/D_2O$ system in our previous study.^{5,9} We performed some experiments in the $C_{16}E_7/H_2O$ system instead of D_2O . The results are qualitatively the same as those for the $C_{16}E_7/D_2O$ system, although the Krafft temperature is a little higher than that of the H_2O system. The fluorescent molecule used is lipophilic tracer DiI, 1,1'-dihexadecyl-3,3,3',3'-tetramethylindocarbocyanine perchlorate (Figure 2, Invitrogen Inc.; excitation and emission wavelengths are 549 and 565 nm, respectively), which enters into bilayers and emits fluorescence from bilayers.

Confocal microscope observation was performed using FV-300 (Olympus Inc.). The excitation laser was a He–Ne green laser whose wavelength is 543 nm. The temperature was controlled by using a hot stage TS62 and controller mk-1000 (Instec Inc.) and was quenched from 16 to 8 $^{\circ}\text{C}$ in the $C_{16}E_7$ system and from 27 to 20 $^{\circ}\text{C}$ in the $C_{16}E_6$ system. Each temperature quench rate was 5 $^{\circ}\text{C}/\text{min}$, and the observation was started simultaneously with a temperature quench.

RESULTS AND DISCUSSION

Figures 3 and 4 show confocal microscope images in the $C_{16}E_7$ and the $C_{16}E_6$ systems, respectively. Each figure was obtained

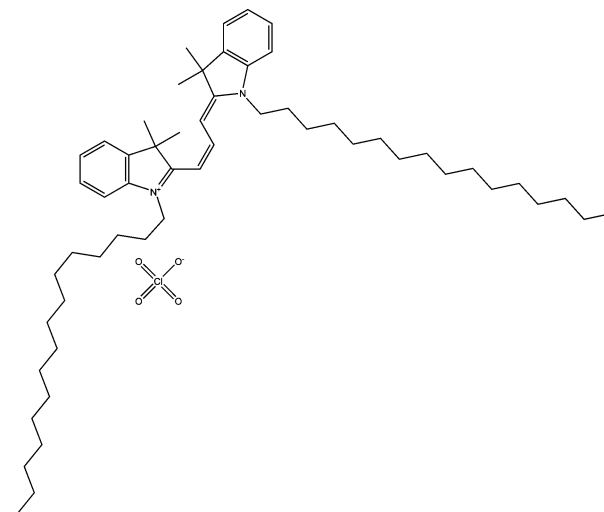


Figure 2. Chemical structure of DiI, 1,1'-dihexadecyl-3,3,3',3'-tetramethylindocarbocyanine perchlorate.

30 min after the temperature quench. The CFM images in the $C_{16}E_7$ system in Figure 3 clearly show spherical vesicles that have a hollow including excess water. The optical microscope image obtained in our previous study cannot distinguish between toroidal aggregates and vesicles with hollows. In this CFM observation, we have confirmed for the first time the existence of spherical vesicles in the $C_{16}E_7$ system. The average size of the vesicles was 2–5 μm , which was estimated from the optical microscope observations, although all of the vesicles were a little deformed from spheres. When the CFM images in Figure 3 were taken, the focal point was set to the vesicles whose diameters were larger than 10 μm because of the technical reason that 3D images of small vesicles are distorted due to the Brownian motion. The shell thickness of the vesicles was about 1.2 μm , and the repeat distance of the stacked bilayers was 7.8 nm.⁵ Then, the number of bilayers was estimated to be about 150.

In the $C_{16}E_6$ system, the structure of the lamellar domain greatly differs from that suggested from the optical microscope observation in our previous study.⁵ Figure 4 clearly shows a randomly arranged network formed by the lamellar domain whose shape is sheet-like instead of string-like, supposed from the optical microscope observation. These sheets may consist of many bilayers. The number of bilayers is about 300, which can be estimated by using the lamellar domain thickness (2.2 μm) and the repeat distance (7 nm). This type of morphology in the $C_{16}E_6$ system has not been reported, and it is surprising that the morphology is quite different from that in the $C_{16}E_7$ system despite the slight difference in hydrophilic length between these two surfactants. To verify the difference between the morphologies in the $C_{16}E_6$ and $C_{16}E_7$ systems, the structural formation processes of these structures were observed by using CFM.

Figures 5 and 6 show the formation processes of domain structures in the $C_{16}E_7$ and $C_{16}E_6$ systems, respectively. For the $C_{16}E_7$ system, we could not observe the time evolution of 3D structures because the 3D images are distorted due to the Brownian motion of small lamellar domains, while we could find a clear vesicle formation process in the 2D images initiated by the growth of very small domains whose size is less than 1 μm at about 225 s after the temperature quench. These small domains could not be observed in the previous microscopy

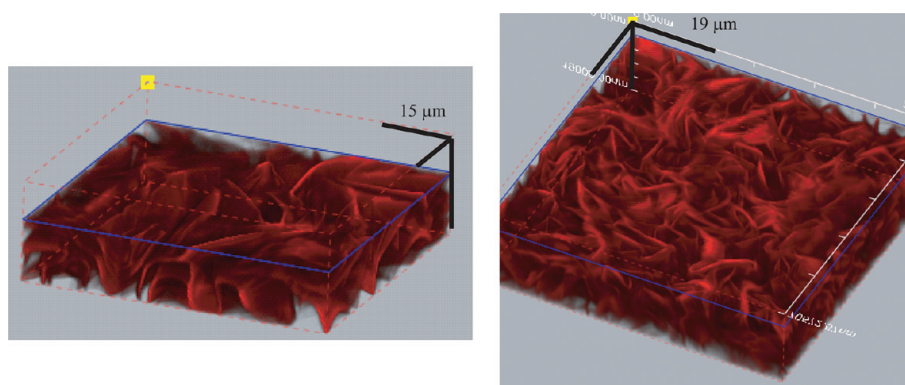


Figure 4. Confocal microscope images at 60 min after temperature quench in the $C_{16}E_6$ system. Lamellar domains are randomly arranged and form network-like structures.

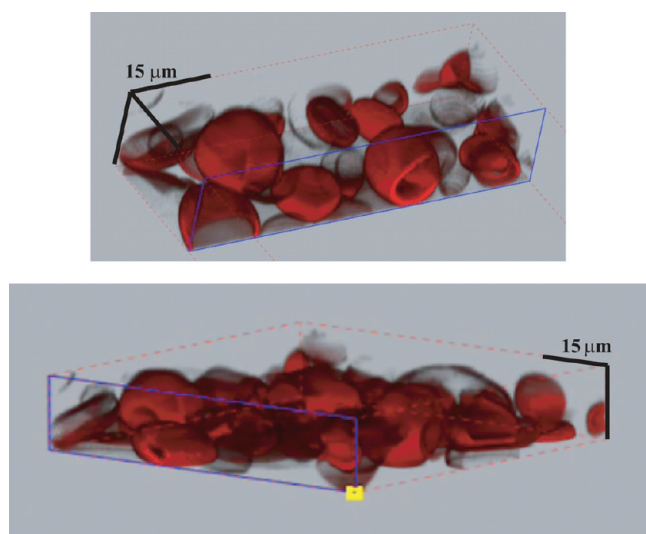


Figure 3. Confocal microscope images at 60 min after temperature quench in the $C_{16}E_7$ system. Round structures with a hollow including excess water, with an average size of about $10\ \mu\text{m}$, can be clearly seen.

experiments. For the initial small lamellar domains, we observed the Bragg peak corresponding to the lamellar structures after 150 s in the previous SAXS results. Therefore, these small domains should already involve the stacked bilayers. About 5 min later, these very small domains grew up to plate-like discoid layers, and they closed to become spherical vesicles. This vesicle formation process is consistent with our previous results observed by optical microscopy^{5,6} and resembles the “standard” pathway, which is established in the case of unilamellar vesicles.^{8,10–14} Especially, it can be explained by the theoretical model, which is expressed by the competition between the edged energy (line tension) and the bending elastic energy (bending modulus) of the disk-like bilayers (unilamellar domains).^{7,8} In the later discussion, we mention this model.

In the $C_{16}E_6$ system, on the other hand, after about 180 s, small discotic lamellar domains rapidly grow up, keeping their shape, and then, they fuse together without closing themselves. After 100 s, lamellar domains are more elongated and densely and randomly arranged in a 3D space. Around 890 s after, the elongation is almost finished, and the structures do not change any more. Although the initial lamellar domains in both systems are discoid, the growth process and the final morphologies are quite different. These differences may be due to difference in

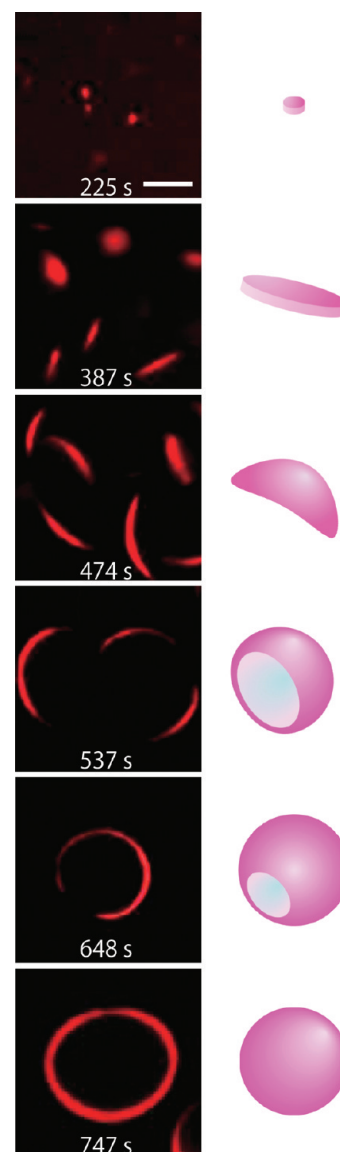


Figure 5. Time evolution of the lamellar domain formations in the $C_{16}E_7$ system. The numbers are the elapsed time from the temperature quench to $8\ ^\circ\text{C}$. The scale bar is $5\ \mu\text{m}$. Very small lamellar domains whose sizes are less than $1\ \mu\text{m}$ appear at about 225 s. About 5 min later, these very small domains grow up to plate-like discoid layers, and they closed to become spherical vesicles.

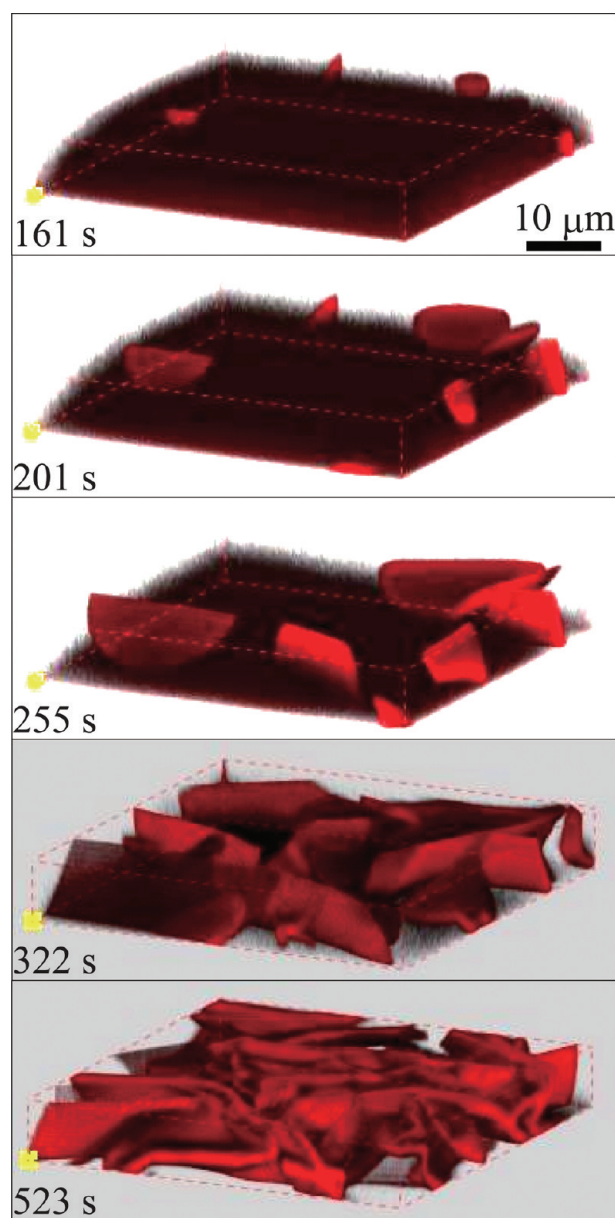


Figure 6. Time elapse of confocal microscope 3D images of the $C_{16}E_6$ system. The numbers are the elapsed time from the temperature quench to 20 °C. At about 180 s, small discotic lamellar domains rapidly grow up, keeping their shape, and they fuse together without closing themselves to form spherical vesicles. After 100 s, lamellar domains are elongated and densely and randomly arranged in 3D space. After around 890 s, the elongation is almost finished, and the structures do not change any more.

the structure of the initial lamellar domains. As shown in Figure 6, the discoid lamellar domain has an edge of layers. The edge part is the more unstable than the planar part because the spontaneous curvature of bilayers is close to zero. Therefore, the discoid lamellar domains transform themselves to reduce the edge parts.

Shioi and Hatton have proposed a simple model for unilamellar vesicle formations in the mixed anion/cation surfactant aqueous solution, taking into account the line tension of the edge parts and the bending modulus of bilayers. For the bilayer with surface area πL^2 and curvature C , the energy of vesicle formation in dimensionless form is expressed

as⁸

$$E' = \frac{(E_{\text{bend}} + E_{\text{edge}})}{2\pi\kappa} = [LC - LC_{\text{sp}}]^2 + (L/\xi)\sqrt{1 - (LC/2)^2} \quad (1)$$

Here, κ is the bending modulus, C_{sp} the spontaneous curvature of the bilayer, λ the line tension, and $\xi = \kappa/\lambda$. For their treatment of the mixed surfactant bilayer, they estimated the finite value of C_{sp} experimentally. In our case of a single-component system, C_{sp} should be zero.⁷ Although the domains in the present systems are multilamellar structures, the structural formations could be qualitatively explained by this model, considering the multilamellar layers as a unilamellar membrane. As shown above, the layers of the $C_{16}E_7$ system (domain thickness) are thinner than those of the $C_{16}E_6$ system. In addition, as shown in the WAXS profile of Figure 7, which

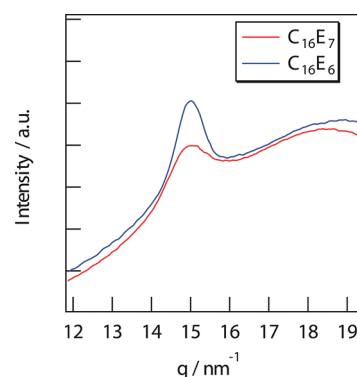


Figure 7. WAXS profiles in the $C_{16}E_6$ and the $C_{16}E_7$ systems. The WAXS peaks at around $q = 15 \text{ nm}^{-1}$ correspond to the surfactant molecules arranged hexagonally in-plane. The peak positions of these two systems are almost the same, which leads to $d = 0.42 \text{ nm}$, whereas the peak width of the $C_{16}E_7$ is broader than that of $C_{16}E_6$.

can give information for bilayer structures on the sub-nanometer scale, the WAXS peaks appear at around $q = 15 \text{ nm}^{-1}$. These peaks correspond to the surfactant molecules arranged hexagonally in a bilayer plane. The peak positions of these two systems are almost the same, which leads to $d = 0.42 \text{ nm}$, whereas the peak width of the $C_{16}E_7$ system (2.21 nm^{-1} (fwhm)) is broader than that in the $C_{16}E_6$ system (1.50 nm^{-1} (fwhm)). This indicates that the molecular packing becomes loose in the $C_{16}E_7$ system due to its large hydrophilic head area. From these results, the bending modulus of the layers in the $C_{16}E_7$ system may be smaller than that in the $C_{16}E_6$ system.

At present, we cannot estimate the line tension from the experimental results. However, from the time evolution of the structural formation in the $C_{16}E_7$ system, the line tension is considered to be relatively low because the discoid lamellar domains are kept for a longer time than that in the $C_{16}E_6$ system. To reduce the edge energy, the flexible layers in the $C_{16}E_7$ system are closed to form vesicles. In the $C_{16}E_6$ system, the discoid domains cannot bend themselves due to their large bending modulus, and they fuse to each other to reduce the edge energy. In order to confirm this scenario, we have investigated the mixed surfactant systems of the $C_{16}E_6$ and $C_{16}E_7$. In the near future, we shall report these results.

■ CONCLUSION

We have studied 3D structures of lamellar domains in aqueous solutions of nonionic surfactants $C_{16}E_6$ and $C_{16}E_7$ below the Krafft temperature by means of confocal microscopy. In the $C_{16}E_6$ system, a new morphology of lamellar domains, randomly arranged network structures, has been found. Their shape is sheet-like instead of string-like, as suggested in our previous study. Also, in the $C_{16}E_7$ system, we have confirmed the existence of spherical vesicles that could not be distinguished with toroidal aggregates in our previous optical microscope observation. The initial formation processes of lamellar domains in these systems have been observed. In the $C_{16}E_6$ system, we have succeeded to observe the 3D structural formation process; the discoid lamellar domains spread to fuse together and form network structures. Taking into account these results and the theoretical model for vesicle formation, it can be deduced that the flexible layers in the $C_{16}E_7$ system are closed to form vesicles to reduce the edge energy. In the $C_{16}E_6$ system, on the other hand, the discoid domains cannot bend themselves due to their large bending modulus, and therefore, they fuse to each other to reduce the edge energy.

■ AUTHOR INFORMATION

Corresponding Author

*E-mail: youheik@tmu.ac.jp.

■ ACKNOWLEDGMENTS

This work was supported by KAKENHI 18068016 (Grant-in-Aid for Scientific Research on Priority Area "Soft Matter Physic") and 21740314 (Grant-in-Aid for Young Scientists (B)) from the Ministry of Education, Culture, Sports, Science and Technology of Japan.

■ REFERENCES

- (1) Kunieda, H.; Shinoda, K. *J. Phys. Chem.* **1976**, *80*, 2468–2470.
- (2) Shinoda, K.; Yamaguchi, N.; Carlsson, A. *J. Phys. Chem.* **1989**, *93*, 7216–7218.
- (3) Yamagata, Y.; Senna, M. *Langmuir* **1999**, *15*, 4388–4391.
- (4) Sasaki, S. *J. Phys. Chem. B* **2007**, *111*, 8453–8458.
- (5) Kawabata, Y.; Matsuno, A.; Shinoda, T.; Kato, T. *J. Phys. Chem. B* **2009**, *113*, 5686–5689.
- (6) Kawabata, Y.; Shinoda, T.; Kato, T. *Phys. Chem. Chem. Phys.* **2011**, *13*, 3484–3490.
- (7) Fromherz, P. *Chem. Phys. Lett.* **1983**, *94*, 259–266.
- (8) Shioi, A.; Hatton, T. A. *Langmuir* **2002**, *18*, 7341–7348.
- (9) Minewaki, K.; Kato, T. *Langmuir* **2001**, *17*, 1864–1871.
- (10) Leng, J.; Egelhaaf, S. U.; Cates, M. E. *Europhys. Lett.* **2002**, *59*, 311–317.
- (11) Weiss, T. M.; Narayanan, T.; Wolf, C.; Gradzielski, M.; Panine, P.; Finet, S.; Helsby, W. I. *Phys. Rev. Lett.* **2005**, *94*, 038303/1–038303/4.
- (12) Weiss, T. M.; Narayanan, T.; Gradzielski, M. *Langmuir* **2008**, *24*, 3759–3766.
- (13) Egelhaaf, S. U.; Schurtenberger, P. *Phys. Rev. Lett.* **1999**, *82*, 2804–2807.
- (14) Nieh, M. P.; Raghunathan, V. A.; Kline, S. R.; Harroun, T. A.; Huang, C. Y.; Pencier, J.; Katsaras, J. *Langmuir* **2005**, *21*, 6656–6661.